Proc. Natl. Acad. Sci. USA
Vol. 91, pp. 2785–2789, March 1994
Biochemistry

Three-dimensional structures of two plant β-glucan endohydrolases with distinct substrate specificities

JOSEPH N. VARGHESE*, THOMAS P. J. GARRETT*, PETER M. COLMAN*, LIN CHEN†, PETER B. HØJ†, AND GEOFFREY B. FINCHER‡

*Biomolecular Research Institute, 343 Royal Parade, Parkville, Victoria, 3052, Australia; †Department of Biochemistry, La Trobe University, Bundoora, Victoria, 3083, Australia; and ‡Department of Plant Science, University of Adelaide, Waite Campus, Glen Osmond, South Australia, 5064, Australia

Communicated by J. E. Varner, October 20, 1993

ABSTRACT **The three-dimensional structures of (1→3)-β-glucanase (EC 3.2.1.39) isoenzyme GII and (1→3,1→4)-β-glucanase (EC 3.2.1.73) isoenzyme EII from barley have been determined by x-ray crystallography at 2.2- to 2.3-Å resolution. The two classes of polysaccharide endohydrolase differ in their substrate specificity and function. Thus, the (1→3)-β-glucanases, which are classified amongst the plant "pathogenesis-related proteins," can hydrolyze (1→3)- and (1→3,1→6)-β-glucans of fungal cell walls and may therefore contribute to plant defense strategies, while the (1→3,1→4)-β-glucanases function in plant cell wall hydrolysis during mobilization of the endosperm in germinating grain or during the growth of vegetative tissues. Both enzymes are α/β-barrel structures. The catalytic amino acid residues are located within deep grooves which extend across the enzymes and which probably bind the substrates. Because the polypeptide backbones of the two enzymes are structurally very similar, the differences in their substrate specificities, and hence their widely divergent functions, have been acquired primarily by amino acid substitutions within the groove.**

Two classes of β-glucan endohydrolases abundant in germinated barley grain are the (1→3)-β-glucan glucanohydrolases (EC 3.2.1.39) and the (1→3,1→4)-β-glucan 4-glucanohydrolases (EC 3.2.1.73) (1, 2). The (1→3)-β-glucanases hydrolyze internal (1→3)-β-glucosidic linkages in β-glucans as follows:

$$\ldots\text{G}3\text{G}\overset{\downarrow}{3}\text{G}3\text{G}\overset{\downarrow}{3}\text{G}3\text{G}3\text{G}\overset{\downarrow}{3}\text{G}3\text{G}3\text{G}\overset{\downarrow}{3}\text{G}3\text{G}3\ldots\text{red},$$

where G represents a glucosyl residue, 3 indicates a (1→3)-β-linkage, and "red" shows the reducing end of the polysaccharide chain. In contrast, the (1→3,1→4)-β-glucanases hydrolyze internal (1→4)-β-glucosyl linkages only in (1→3,1→4)-β-glucans in which the glucosyl residue involved in the glycosidic linkage cleaved is substituted at the C(O)3 position, as follows:

$$\ldots\text{G}4\text{G}3\text{G}\overset{\downarrow}{4}\text{G}4\text{G}3\text{G}\overset{\downarrow}{4}\text{G}4\text{G}4\text{G}3\text{G}\overset{\downarrow}{4}\text{G}4\text{G}3\ldots\text{red},$$

where 4 represents a (1→4)-β-linkage. The (1→3,1→4)-β-glucanases have no action on (1→3)-β-glucans such as callose, nor do the (1→3)-β-glucanases hydrolyze plant cell wall (1→3,1→4)-β-glucans in which contiguous (1→3)-β-glucosyl residues are absent (1, 2).

(1→3)-β-Glucanases are important representatives of the "pathogenesis-related" (PR) group of proteins expressed when plants are subjected to microbial attack and are widely distributed in higher plants (3). The enzymes have been implicated in the protection of plants against potential pathogens through their ability to hydrolyze the (1→3)- and (1→3,1→6)-β-glucans commonly found in fungal cell walls, although the fungal polysaccharide must contain tracts of contiguous, unsubstituted (1→3)-β-glucosyl residues before hydrolysis will occur (4). The (1→3,1→4)-β-glucanases have a quite distinct function. They are essential for the depolymerization of plant cell wall β-glucans in germinating grain and in young vegetative tissues (5).

Evidence is accumulating that, despite their distinct substrate specificities, the (1→3)- and (1→3,1→4)-β-glucanases are encoded by genes which originated by duplication of a common ancestral gene (2, 5). The encoded enzymes exhibit approximately 50% positional identity in amino acid sequence and are similar in length (2, 6), and their catalytic amino acids occupy highly conserved positions in the primary structure of the enzymes (7). We recently crystallized the (1→3,1→4)-β-glucanase isoenzyme EII and (1→3)-β-glucanase isoenzyme GII from barley (8) and have now solved their three-dimensional structures to 2.2- and 2.3-Å resolution, respectively.§ The similarity of the two structures suggests that the distinct substrate specificities can be acquired by the alteration of amino acid side chains in the substrate-binding groove, with little or no main-chain adjustment.

MATERIALS AND METHODS

Data Collection. The space group and cell dimensions for the crystallized (1→3,1→4)-β-glucanase isoenzyme EII are $P4_32_12$, $a = b = 87.4$ Å, $c = 109.5$ Å and for the (1→3)-β-glucanase isoenzyme GII are $P3_221$, $a = b = 86.9$ Å, $c = 156.0$ Å, as previously described (8). For each native enzyme and for one derivative (HgOAc) diffraction data to 1.8 Å were collected at the Photon Factory (Tsukuba, Japan), using the Weissenberg method (9). For the (1→3,1→4)-β-glucanase, more native data and the remaining derivative data sets were collected with a Siemens multiwire detector or with a Mar Research image plate detector. Statistics for the integrated (10–12) and merged (13) data are summarized in Table 1.

(1→3,1→4)-β-Glucanase Structure Solution and Refinement. The structure of the (1→3,1→4)-β-glucanase was determined by J.N.V., using the multiple isomorphous replacement (MIR) method. The locations of the heavy atom sites were determined by difference Patterson and difference Fourier methods. The heavy atom parameter refinement and MIR phasing resulted in an overall figure of merit of 0.56 to 3-Å resolution using 7976 reflections. The enantiomorph was determined by including the anomalous scattering data of the HgOAc derivative.

A 3-Å electron density map was calculated by using the MIR phases, including anomalous data from the HgOAc derivative. The image was then filtered by using the method

The publication costs of this article were defrayed in part by page charge payment. This article must therefore be hereby marked "*advertisement*" in accordance with 18 U.S.C. §1734 solely to indicate this fact.

Abbreviation: MIR, multiple isomorphous replacement.

§The atomic coordinates have been deposited in the Protein Data Bank, Chemistry Department, Brookhaven National Laboratory, Upton, NY 11973 [references 1GHS and 1GHR for the (1→3)-β-glucanase and (1→3,1→4)-β-glucanase, respectively].

Table 1. Collection statistics of data for native and heavy metal derivatives of barley β-glucanases

Crystal	Number of observations	Number of reflections	⟨*R*(sym)⟩	*R*(merge)	Resolution, Å
(1→3)-β-Glucanase					
Native	114,164	32,509	6.0	9.8	1.8
(1→3,1→4)-β-Glucanase					
Native	86,286	16,399	5.5	10.1	1.8
HgOAc	43,660	12,787	7.1	8.8	1.8
K_2PtCl_4a	13,820	5,598	7.8	11.1	2.8
K_2PtCl_4b	10,112	6,243	5.0	5.0	2.4
$Pt(NH_3)_2(NO_2)_2$	14,876	6,566	6.2	8.2	2.4

All derivatives were prepared by soaking crystals in heavy atom solutions with standard buffer (100 mM Tris·HCl, pH 7.5): 2 mM HgOAc, 24-h soak; the two $PtCl_4$ derivatives were 10 mM, 48-h soak and 10 mM, 36-h soak; 10 mM (saturated) $Pt(NH_3)_2(NO_2)_2$ was a 60-day soak. *R*(merge) = $\Sigma(I_i - \langle\Sigma I\rangle)/I_i$ summed over all independent reflections and *R*(sym) measures the agreement of multiple measurements of intensity within each frame of data.

of Wang (14), and the resulting electron density map was of sufficient quality to trace the polypeptide chain of almost all of the protein, determine the direction of the α-helices, and identify the fold as an eight-stranded α/β-barrel.

An atomic model of the protein was built from the C^α coordinates with the computer graphics package O (15). For some of the loops and for the COOH terminus ambiguous or weak density was resolved by comparison with the (1→3)-β-glucanase isoenzyme GII structure. The atomic model was refined by using the XPLOR package (16) and the atomic restraint parameters of Engh and Huber (17). Initially, energy minimization was used, and at 2.8-Å resolution the model was subjected to a full simulated annealing refinement procedure (18) and the resulting model was reappraised by computer graphics. The resolution was extended to 2.2 Å, and individual temperature factors were included in the refinement. Electron density consistent with a carbohydrate moiety at N190 (19) was observed but not modeled. Cis peptides were observed preceding P137 and A276. A total of 45 water molecules were added where difference Fourier peaks above 5 σ were found to have an environment consistent with water hydrogen bonding. The final crystallographic *R*-factor was 0.176 [for data 6–2.2 Å and $I \geq 2\sigma(I)$], and the rms deviations from ideal bond lengths and angles were 0.012 Å and 1.62°, respectively.

(1→3)-β-Glucanase Structure Solution and Refinement. The structure of (1→3)-β-glucanase was determined by T.P.J.G., using the molecular replacement method (20) and the MERLOT package (21). A self-rotation function was calculated and was found to be consistent with a pseudo point group of *P*6/mmm and two molecules per asymmetric unit. At this stage a high-quality electron density map for the (1→3,1→4)-β-glucanase had been obtained although no atomic model had been built. Therefore, the electron density of the (1→3,1→4)-β-glucanase was used as the search model. Cross-rotation functions were calculated for data in various resolution ranges. Two pairs of potential solutions, each consistent with the self-rotation function, were found and refined, using a fine grid search. Translation functions for the crystallographic threefold relation were calculated for each pair of potential solutions, using the same data ranges as before. In functions using data 8–3.5 Å, the highest peaks in each case occurred on the $w = 1/3$ section (7.3 and 7.6 standard deviations, respectively), indicating a space group of $P3_221$. The remaining positional parameters were determined from additional translation functions and the orientation parameters for both molecules were refined by a stepwise local search for the minimum *R* factor.

A model electron density for the asymmetric unit of the (1→3)-β-glucanase was constructed from the MIR density for the (1→3,1→4)-β-glucanase. The resulting "calculated" data, which were completely independent of an atomic model, formed the starting point for the phase improvement by density averaging (22) using Sim-weighted F_o maps. The initial figure of merit was 0.54 and $R = 0.470$ for data 10–3 Å. After 20 cycles of averaging the figure of merit was 0.77, $R = 0.188$, and the rms shift from the original phases was 78°. The resulting averaged electron density map appeared not to be biased to the starting density, as illustrated by clear density for amino acids in the regions of insertions and deletions and for sequence differences such as Phe to Ile. At this stage main-chain atoms for two-thirds of the amino acids of the (1→3,1→4)-β-glucanase had been placed in density, and this model was transformed into the (1→3)-β-glucanase map. From this point the electron density maps for both enzymes were traced concurrently. One molecular model was constructed for the (1→3)-β-glucanase, using density from both molecules superimposed.

Initially, two molecules were refined as rigid bodies, using data 7–3.2 Å. Strict noncrystallographic symmetry was imposed and the structure was refined by energy minimization to 2.6-Å resolution. A simulated annealing protocol was now used and from 2.5-Å resolution noncrystallographic symmetry constraints were removed, the first water molecules were added, and isotropic thermal parameters were refined. In both molecules cis peptides were found preceding P82, P138, and A275. Upon completion of the refinement, $R = 0.179$ [for data 6–2.3 Å and $I \geq 2\sigma(I)$], the rms deviations from ideal bond lengths and angle were 0.013 Å and 1.68°, respectively, and the rms deviation in C^α positions for the two molecules was 0.30 Å.

RESULTS AND DISCUSSION

Description of the Structures. The (1→3)-β-glucanase and (1→3,1→4)-β-glucanase structures have essentially identical α/β-barrel folds (23). Minor perturbations are found in the loops, mainly at positions where there are sequence insertions and deletions (Figs. 1 and 2). A deep groove runs north–south along the full length of the upper surface of the molecule, perpendicular to the barrel axis, and is suggestive of a site to which the polysaccharide substrate might be bound.

The NH_2 terminus lies under the molecule, with the polypeptide entering the east side of the barrel as β_1 (for notation see Fig. 1). The chain emerges on the upper surface, turns back towards the bottom surface as α_1, and, after traversing the outside of the molecule, meets β_2. This motif is repeated for strands β_2–β_4, building the upper half of a conventional α/β-barrel. For the third α/β loop there are two helices (Fig. 2 *Upper*). The lower half of the barrel has more elaborate secondary structural elements that have not been observed previously in α/β-barrel structures. There is a "subdomain" which is built around helix α_6 and which runs perpendicular to the groove axis at the southern end of the groove. It is supported by three two-stranded antiparallel β-sheet "fingers" (B_5 on the upper surface, B_7 on the lower

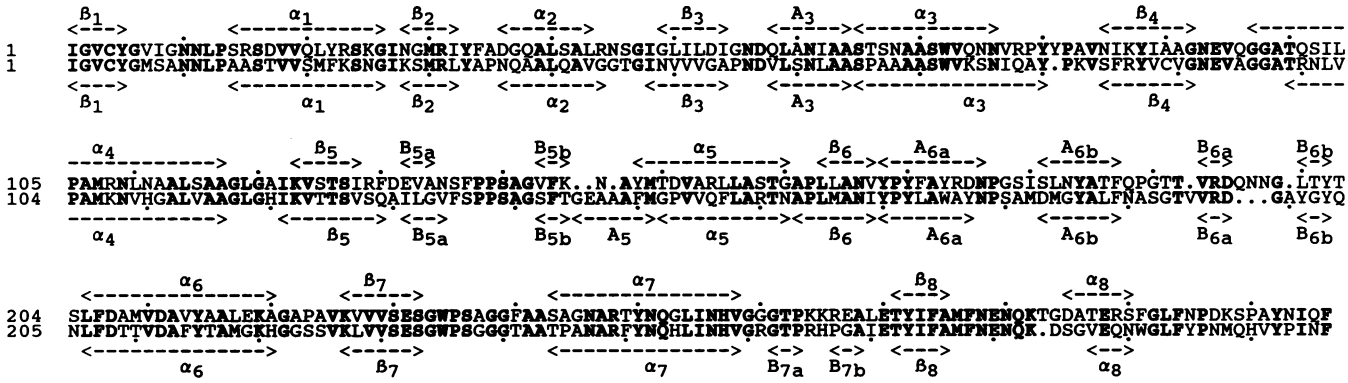

FIG. 1. Sequence comparison of the (1→3)-β-glucanase isoenzyme GII (upper line) and the (1→3,1→4)-β-glucanase isoenzyme EII (lower line) based on the three-dimensional structure. Residues common to both enzymes are in bold, and numbers are given for the first residue of each line. The secondary structural elements of both enzymes are given above the (1→3)-β-glucanase sequence and below the (1→3,1→4)-β-glucanase sequence. The β-barrel strands are referred to as β_i and the major (longest) helices connecting the β strands as α_i, where i is in the range 1–8. Minor β-sheet and α-helices are referred to as B_i and A_i, respectively, if they appear after the strand β_i and before β_{i+1} and a further subscript a or b is added if more than one minor structure occurs.

surface, and B_6 at the southern end of the groove) and three small helices (A_5 at the western side and A_{6a} and A_{6b} at the eastern side of the groove). This subdomain, which forms a platform for the residues making up the lower half of the groove, differs in detail between the (1→3,1→4)-β-glucanase and the (1→3)-β-glucanase (Fig. 2 *Upper* and *Lower Right*); for example, the helix A_5 is missing in the (1→3)-β-glucanase.

The COOH-terminal segment, consisting of some 30 residues, starts after the strand β_8 and has an unusual turn involving a cis peptide bond between residues F274 (F275) and A275 (A276).¶ A *cis*-proline could not accommodate this type of turn, which governs the positioning of F274 (F275) in the catalytic site and the conformation of the loop of residues from 275 to 286 (276 to 286). The COOH-terminal segment then finds its way down to the underside of the molecule between the helices α_1 and α_7, and finishes within 4.2 Å of the NH_2 terminus.

The α/β-barrel fold of these barley β-glucanases does not appear to fit in the classification devised by Farber and Petsko (24). Although there are some similarities with the α-amylase family in that β_1 is near the major axis of the barrel, no divalent metal ion is observed in the structures and, indeed, none appears to be required for activity (1). Cellobiohydrolase II, a fungal β-glucan exohydrolase, has a fold similar to but different in detail from the barley enzymes (25), but microbial (1→4)-β-glucan endohydrolases (cellulases) have completely different structures (26, 27).

Substrate-Binding and Catalytic Sites. The most obvious structural feature of the barley (1→3)- and (1→3,1→4)-β-glucanases is a deep cleft approximately 40 Å long (Fig. 3), running parallel to the major axis of each molecule and over the COOH-terminal face of the β-barrel. At the northern end (Fig. 2 *Upper*) is a broad opening where the cleft runs over the short β_2-α_2 loop. At the other end there is a longer, narrower exit between the COOH-terminal loops of strands β_5 and β_6. Here the transverse helix α_6 and a short β-ribbon form an extension to the canonical α/β-barrel. The length of the cleft is sufficient to accommodate 7 or 8 residues of extended (1→4)- or (1→3)-β-glucan chains, respectively. Mapping of the substrate-binding region of the (1→3)-β-glucanase also indicates that subsites for eight glucosyl residues are present (M. Hrmova and G.B.F., unpublished results).

The two catalytic glutamic residues E231 (E232) and E288 (E288) (7) lie about one-third of the way down the cleft and a little to the right of the barrel axis (Fig. 2 *Lower Right*). These two residues adopt very similar conformations in the two enzymes, and the distance between O^{ε} atoms is 8.2 Å in each case. If it is assumed that the glycosidic oxygen is positioned between these two residues, the distance is consistent with the proposed mechanism of hydrolysis, in which protonation of the glycosidic oxygen by the catalytic acid residue is followed by stabilization of the intermediate oxycarbonium ion by the catalytic nucleophile (28).

The catalytic nucleophile, E231 (E232), sits at the bottom of the cleft and the O^{ε} atoms are held in position by hydrogen bonds to the O^{η} atoms of Y33 (Y33) and Y168 (Y170). Residue E231 (E232) is mostly buried, and only the end of the carboxylate group contributes to the surface of the cleft (Fig. 2 *Lower Right*). The catalytic acid, E288 (E288), sits near the lip of the cleft within the loop of residues 279–288 (280–288). Although the loops have different conformations (Fig. 2 *Lower Right*), each E288 residue occupies a very similar position. No hydrogen bonding occurs between the carboxylate of E288 (E288) and any other atom of the protein, consistent with the role of E288 as a proton donor (7). Interaction of E288 with solvent has not been ruled out, but details will not be available until further crystallographic refinement has been performed.

Surrounding E231 (E232) and extending to E288 along the surface of the substrate-binding cleft is a cluster of amino acid residues which are highly conserved in the sequences of these and other plant (1→3)- and (1→3,1→4)-β-glucanases (6). At the floor of the cleft on the western side are N93 (N92), E94 (E93), and N166 (N168), which form a hydrogen-bonded network and which would sterically restrict the movement of E231 (E232). Furthermore, the N93 (N92) and E94 (E93) residues probably form hydrogen bonds with the substrate during binding. On the eastern wall of the cleft between the catalytic glutamates, there is a predominantly hydrophobic surface formed by Y168 (Y170), F171 (L173), F291 (W291), and F274 (F275) and extending to Y33 (Y33) (Fig. 2 *Lower Right*). This surface is in an appropriate position for a hydrophobic contact with the faces of glucosyl residues. Minor differences in amino acid residues at F171 (L173) and F291 (W291) may also influence substrate specificity.

Adjacent to the E288 residues (Fig. 2 *Lower Right*) are the strictly conserved residues K282 (K283) and E279 (E280). These residues appear to be important in influencing the protonation state of the catalytic acid E288. The catalytic acid, which acts as a proton donor during hydrolysis, should

¶Throughout this discussion, residue numbers are for the (1→3)-β-glucanase, with corresponding numbers for the (1→3,1→4)-β-glucanase in parentheses.

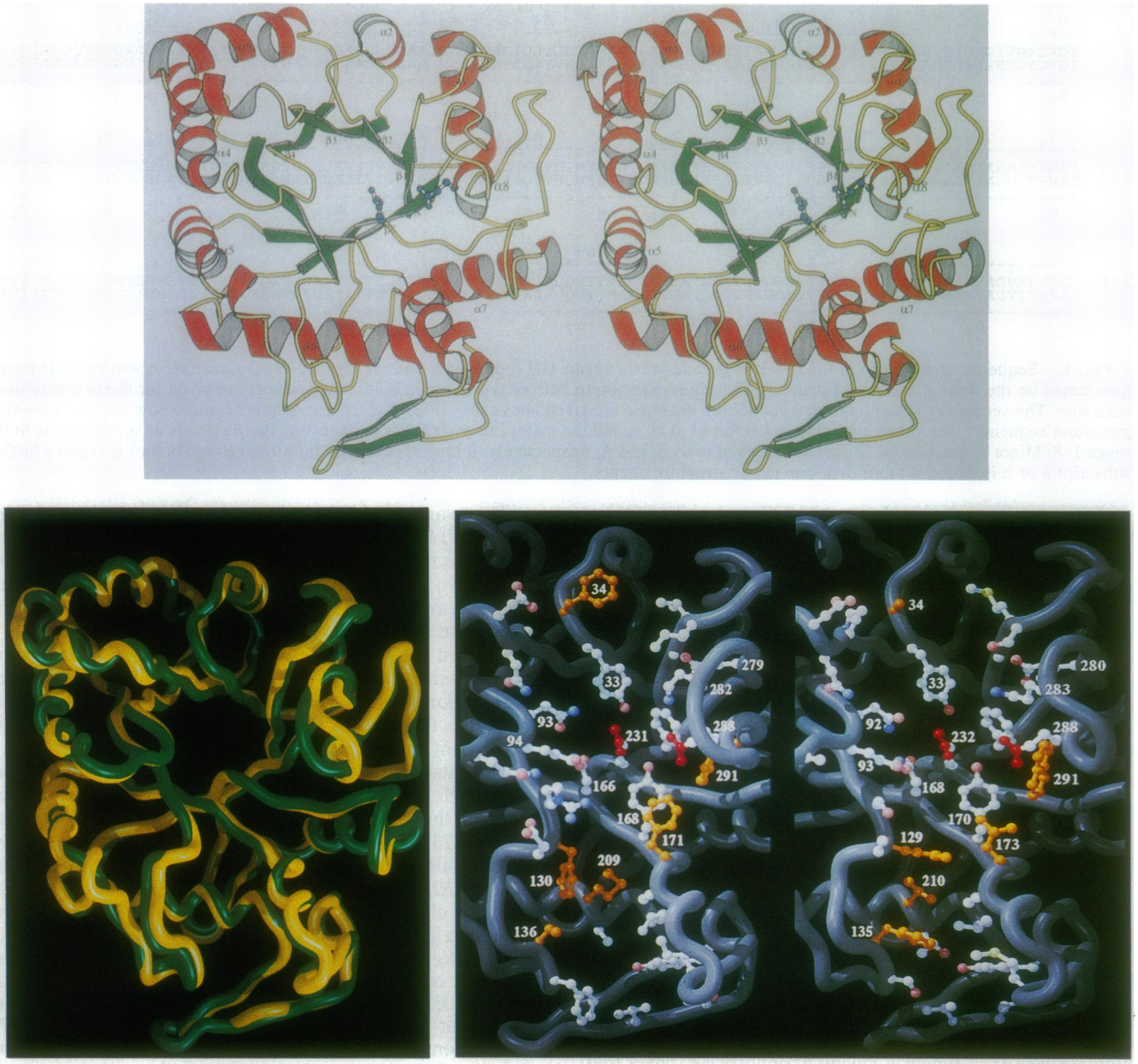

FIG. 2. (*Upper*) Schematic stereoview of the (1→3,1→4)-β-glucanase isoenzyme EII, showing secondary structure. α-Helices are drawn as red curled tape, β-strands as green arrows, and the remainder as yellow rope. Some small β-strands are not shown. The catalytic glutamic residues E232 and E288 are shown in blue. (*Lower Left*) Superposition of the polypeptide backbone of the (1→3)-β-glucanase isoenzyme GII (green) and (1→3,1→4)-β-glucanase isoenzyme EII (gold) in the same orientation as *Upper*. The rms deviation in C^{α} positions between the (1→3,1→4)-β-glucanase and each molecule of (1→3)-β-glucanase is 0.65 Å for 278 residues. (*Lower Right*) Catalytic grooves of the (1→3)-β-glucanase (left) and the (1→3,1→4)-β-glucanase (right) in the same orientation as *Upper*. The catalytic carboxylates are shown in red and the amino acids which could affect substrate specificity are in orange (see text for details). Side chains of other amino acids which line the grooves are colored by atom type: C, white; N, pale blue; O, pink; and S, pale yellow.

have a pK_a significantly higher than other glutamic residues, because it must be capable of proton exchange in the pH range 4.5–6.0, where maximal activity occurs (7). The close proximity of E279 (E280) to E288 (E288) may give rise to elevated pK_a values for these residues. It has been suggested that R145 in phage T4 lysozyme and a helix dipole in hen egg white lysozyme are needed to stabilize a negative charge on the proton donor during catalysis (29). If so, K282 (K283) could play this role in the barley β-glucanases.

Determinants of Substrate Specificity. Towards both ends of the cleft, beyond the conserved patch that surrounds the catalytic amino acid residues, there are amino acid differences which probably account for the differences in substrate specificity of the two barley β-glucanases. At the northern end of the cleft in the (1→3)-β-glucanase there is residue F34, which is replaced by the much smaller A34 in the (1→3,1→4)-β-glucanase (Fig. 2 *Lower Right*); in other (1→3)-β-glucanases this residue usually contains a large side chain (6). At the other end of the cleft the (1→3,1→4)-β-glucanase has a glutamine at position 129 and a phenylalanine at 135, and these residues lie across the floor to effectively block the bottom of the cleft (Fig. 2 *Lower Right*). The amide of Q129 forms hydrogen bonds with the main chain on the opposite side of the cleft and the small T210 from α_6 leaves a small gap between Q129 and F135. In the (1→3)-β-glucanase, the equivalent residues, F130 and S136, sit out of the way of substrate binding, but M209 from α_6 of the (1→3)-β-glucanase is larger than T210 of the (1→3,1→4)-β-glucanase and provides an obstruction further along the cleft (Fig. 2 *Lower Right*). When a (1→3)-β-glucan is positioned in the catalytic

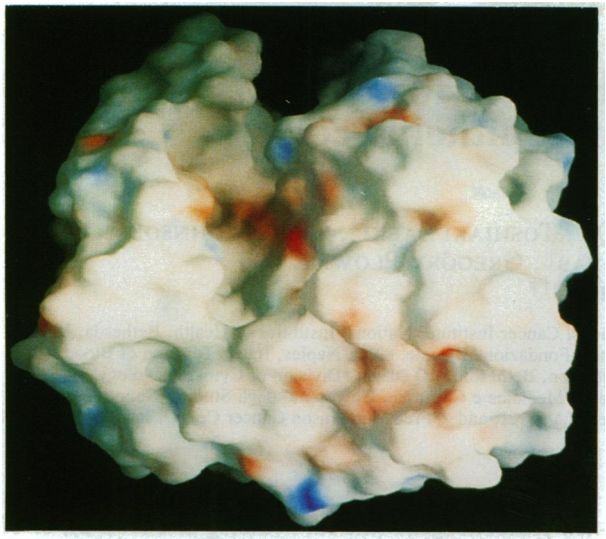

FIG. 3. Molecular surface drawing of (1→3)-β-glucanase isoenzyme GII, colored according to electrostatic potential (blue, positive; red, negative). The enzyme is viewed from the northern end of the molecule as shown in Fig. 2 and shows the deep substrate-binding groove. The position of E231 is indicated by a pink region in shadow at the bottom of the groove (center left).

site of the (1→3)-β-glucanase, it is possible to place a glucosyl residue edgewise in the cleft in the space vacated by Q129 of the (1→3,1→4)-β-glucanase. Thus, the (1→3)-β-glucanase cleft could accommodate its substrate in this manner, but Q129 would prevent the (1→3)-β-glucan from binding in the cleft of the (1→3,1→4)-β-glucanase.

Evolution of β-Glucanase Structure and Function. Recent crystallographic evidence shows that a (1→3,1→4)-β-glucanase from *Bacillus* spp. exhibits a "jelly-roll" β-barrel structure (30), which is quite different from the α/β-barrel structure of the barley (1→3,1→4)-β-glucanase described here (Fig. 2 *Upper*). Clearly, the identical substrate specificities of the bacterial and plant (1→3,1→4)-β-glucanases must have arisen by convergent evolution. In contrast, the (1→3,1→4)- and (1→3)-β-glucanases in higher plants appear to have originated by divergent evolution from a common ancestral enzyme. This was initially suggested by similarities in gene structure and amino acid sequence between the two classes of plant β-glucan endohydrolases (2, 6), and by the conservation of catalytic amino acid residues (7). Evidence in favor of a common ancestry has now been strengthened by the similar three-dimensional structures of the barley (1→3)-β-glucanase and (1→3,1→4)-β-glucanase (Fig. 2 *Lower Left*). The evolution of substrate specificity appears to have been possible simply through limited amino acid substitutions rather than through large-scale changes in the main-chain conformation. Nevertheless, the amino acid substitutions have permitted a dramatic shift in function, so that different classes of enzymes derived from a single multigene family can specifically hydrolyze related but quite distinct polysaccharides found in cell walls of fungi or higher plants.

We are indebted to Prof. B. A. Stone for his assistance and advice. We thank Prof. N. Sakabe and the National Laboratory for High Energy Physics, Tsukuba, Japan, for access to the data collection facilities at the Photon Factory and A. van Donkelaar for technical assistance. This work was supported in part by grants to P.B.H., P.M.C., and G.B.F. from the Australian Research Council. Financial assistance from the Australian National Beamline Facility is gratefully acknowledged. T.P.J.G. is an Australian Research Council QEII Fellow.

1. Woodward, J. R. & Fincher, G. B. (1982) *Eur. J. Biochem.* **121**, 663–669.
2. Høj, P. B., Hartman, D. J., Morrice, N. A., Doan, D. N. P. & Fincher, G. B. (1989) *Plant Mol. Biol.* **13**, 31–42.
3. Dixon, R. A. & Lamb, C. J. (1990) *Annu. Rev. Plant Physiol. Plant Mol. Biol.* **41**, 339–367.
4. Hrmova, M. & Fincher, G. B. (1993) *Biochem. J.* **289**, 453–461.
5. Slakeski, N., Baulcombe, D. C., Devos, K. M., Doan, D. N. P. & Fincher, G. B. (1990) *Mol. Gen. Genet.* **224**, 437–449.
6. Xu, P., Wang, J. & Fincher, G. B. (1992) *Gene* **120**, 157–165.
7. Chen, L., Fincher, G. B. & Høj, P. B. (1993) *J. Biol. Chem.* **268**, 13318–13326.
8. Chen, L., Garrett, T. J. P., Varghese, J. N., Fincher, G. B. & Høj, P. B. (1993) *J. Mol. Biol.* **234**, 888–889.
9. Sakabe, N. (1991) *Nucl. Instrum. Methods Phys. Res. Sect. A* **303**, 448–463.
10. Rossmann, M. G. (1979) *J. Appl. Crystallogr.* **12**, 225–238.
11. Howard, A. J., Nielsen, C. & Xuong, Ng, H. (1987) *Methods Enzymol.* **114**, 452–472.
12. Higashi, T. (1989) *J. Appl. Crystallogr.* **22**, 9–18.
13. Steigeman, W. (1974) Dissertation (Technical Univ. Munich).
14. Wang, B. C. (1985) *Methods Enzymol.* **115**, 90–112.
15. Jones, T. A., Zou, J. Y. & Kjeldgaard, M. (1991) *Acta Crystallogr. Sect. A Found. Crystallogr.* **47**, 110–119.
16. Brünger, A. T. (1992) X-PLOR (Yale Univ. Press, New Haven, CT), Version 3.3.
17. Engh, R. A. & Huber, R. (1991) *Acta Crystallogr. Sect. A. Found. Crystallogr.* **47**, 392–400.
18. Brünger, A. T. (1988) *J. Mol. Biol.* **203**, 803–816.
19. Doan, D. N. P. & Fincher, G. B. (1992) *FEBS Lett.* **309**, 265–271.
20. Rossmann, M. G., ed. (1972) *The Molecular Replacement Method* (Gordon & Breach, New York).
21. Fitzgerald, P. M. D. (1988) *J. Appl. Crystallogr.* **21**, 273–278.
22. Bricogne, G. B. (1976) *Acta Crystallogr. Sect. A Found. Crystallogr.* **32**, 832–847.
23. Banner, D. W., Bloomer, A. C., Petsko, G. A., Phillips, D. C., Pogson, C. I., Wilson, I. A., Corran, P. H., Furth, A. J., Milman, J. D., Offord, R. E., Priddle, J. D. & Waley, S. G. (1975) *Nature (London)* **255**, 609–614.
24. Farber, K. G. & Petsko, G. A. (1990) *Trends Biochem. Sci.* **15**, 228–234.
25. Rouvinen, J., Bergfors, T., Teeri, T., Knowles, J. K. C. & Jones, T. A. (1990) *Science* **249**, 380–386.
26. Juy, M., Amit, A. G., Alzari, P. M., Poljak, R. J., Claeyssens, M., Beguin, P. & Aubert, J.-P. (1992) *Nature (London)* **357**, 89–91.
27. Davies, G. J., Dodson, G. G., Hubbard, R. E., Tolley, S. P., Dauter, Z., Wilson, K. S., Hjort, C., Mikkelson, J. M., Rasmussen, G. & Schulein, M. (1993) *Nature (London)* **365**, 362–364.
28. Svennson, B. & Søgaard, M. (1993) *J. Biotechnol.* **29**, 1–37.
29. Strynadka, N. C. J. & James, M. N. G. (1991) *J. Mol. Biol.* **220**, 401–424.
30. Keitel, T., Simon, O., Borriss, R. & Heinemann, U. (1993) *Proc. Natl. Acad. Sci. USA* **90**, 5287–5291.